Eur. Phys. J. A **18**, 93–102 (2003)
DOI 10.1140/epja/i2003-10041-3

THE EUROPEAN PHYSICAL JOURNAL A

Prompt fission neutron spectra of ^{238}U(n, f) above emissive fission threshold

V.M. Maslov[1,a], Yu.V. Porodzinskij[1], M. Baba[2], A. Hasegawa[3], N. Kornilov[4], A.B. Kagalenko[4], and N.A. Tetereva[1]

[1] Joint Institute for Nuclear and Energy Research, 220109, Minsk-Sosny, Belarus
[2] Cyclotron and Radioisotope Center, Tohoku University, Sendai, Japan
[3] Department of Nuclear Energy System, Tokai Research Establishment, Japan Atomic Energy Research Institute, Tokai-mura, Naka-gun, Ibaraki-ken, Japan
[4] SSC RF Institute of Physics and Power Engineering, Obninsk, Russia

Received: 3 February 2003 / Revised version: 24 April 2003 /
Published online: 9 October 2003 –
Communicated by C. Signorini

Abstract. Model calculations were performed to interpret prompt fission neutron spectra (PFNS) of the ^{238}U(n, f) reaction for incident neutron energies E_n = 6–18 MeV. Pre-fission (pre-saddle) ^{238}U(n, $x$nf) reaction neutron spectra were calculated with Hauser-Feshbach statistical model, ^{238}U fission and (n, xn) reaction cross-section data being described consistently. The increase of the cut-off energy of (n, nf) reaction neutron spectra with excitation energy of fissioning nucleus is described. For E_n = 6–9 MeV the low-energy PFNS component, which is due to the contribution of pre-fission (n, nf) neutrons, is compatible with measured data. Average energy of prefission (n, nf) neutrons is shown to be rather dependent on E_n. For E_n = 13–18 MeV, a decrease of measured PFNS average neutron energies is interpreted. Spectra of neutrons, evaporated from fission fragments, were approximated as a sum of two Watt distributions. The reduced fission fragment velocity is assumed for the neutron emission during fragment acceleration. Several interpretations of observed soft neutron excess are investigated, *i.e.*, possible uncertainties of emissive fission contributions and additional neutron source. We claim the soft neutron excess cannot be attributed to the ^{238}U(n, $x$nf) pre-saddle neutrons contribution.

PACS. 25.85.Ec Neutron-induced fission

1 Introduction

Extensive investigations of prompt fission neutron spectra (PFNS) by Boykov *et al.* [1,2], Smirenkin *et al.* [3] and Lovchikova *et al.* [4] below and above emissive fission thresholds for the ^{238}U(n, f) reaction were accomplished recently. It was observed that for incident neutron energies $E_n \sim$ 13–18 MeV average energy values of PFNS $\langle E \rangle$ were lower than estimates based on previous experimental data [5–8] and theoretical-approach [9] predictions. This discrepancy invoked the speculations that modelling of prompt fission neutron emission from fission fragments in multiple-chance fission reaction, pre-fission (or, equivalently, pre-saddle) (n, $x$nf) neutron emission included, cannot reproduce the low-energy part of PFNS. The experimental investigations triggered assumptions that some fission neutrons could be emitted from non-accelerated fission fragments (see Svirin *et al.* [10]). However, several alternative explanations of the lowering of average prompt fission neutron energies $\langle E \rangle$ look feasible.

In neutron-induced fission of ^{238}U target nuclide, on the path of the composite nucleus ^{239}U to the scission point several neutron-emitting sources could be distinguished. Pre-equilibrium neutron could be emitted before a composite nucleus ^{239}U attains thermal equilibrium, it is obviously a pre-saddle neutron. When incident neutron energy is higher than the threshold of (n, nf) emissive fission reaction ($E_{nnf} \sim$ 6 MeV), more pre-saddle neutrons might be evaporated before a composite system attains saddle-point deformation. Upon reaching saddle deformation the nucleus rapidly transits from the saddle point to the "scission" point. Though this saddle-to-scission time is rather short ($\sim 10^{-21}$ s) [11] "pre-scission" neutrons still could be emitted [12]. Notwithstanding the type of the neutrons, emitted before the fissioning U nucleus reaches the scission point, either they are pre-saddle, or pre-scission, fission reaction looks like multiple-chance fission. After scission, primary fission fragments may emit neutrons as well. Most of the neutrons are emitted from the fragments after their full acceleration in mutual Coulomb field. It was shown by Knitter *et al.* [13] that this happens

[a] e-mail: maslov@sosny.bas-net.by

within $\sim 10^{-18}$–10^{-17} s. It might be assumed that some neutrons could be emitted just after scission [14], *i.e.* before full acceleration of the fragments. We will analyze measured PFNS data for the ^{238}U(n, f) reaction above and below the emissive fission threshold and interpret major data trends in terms of pre-saddle and post-fission neutron spectra. Previously (n, $x$nf) neutrons spectra were predicted semi-quantitatively [10,15,16]. We will estimate the contribution of (n, $x$nf) pre-fission neutrons to the measured PFNS in a more reliable way, *i.e.*, using Hauser-Feshbach statistical model calculations, based on the description of ^{238}U(n, f), ^{238}U(n, 2n) and ^{238}U(n, 3n) reaction cross-sections [17,18]. We will define the upper level of possible deficiency of soft neutrons and attribute it to the influence of various factors, that may change post-fission neutron spectra.

2 PFNS data analysis

Average energies $\langle E \rangle$ of PFNS for the ^{238}U(n, f) reaction *versus* incident neutron energy $E_{\rm n}$ are shown in fig. 1. Up to $E_{\rm n} \sim 10$ MeV $\langle E \rangle$ data, extracted from the measured PFNS are roughly consistent, while above ^{238}U(n, 2nf) emissive fission threshold ($E_{\rm n} \sim 13$ MeV) they scatter by ~ 500 keV. Though calculated and evaluated $\langle E(E_{\rm n}) \rangle$ curves remain inside this data spread, the uncertainty makes ambiguous the PFNS shape estimates for ^{238}U and other actinide target nuclei. Analysis of PFNS measured data might be of help to select reliable PFNS data sets. We will briefly analyze relevant experimental methods, their reliability and possible systematic errors.

Prompt fission neutron spectra for ^{238}U(n, f) reaction were measured with two different methods. In a simpler one, rather massive ^{238}U target samples (~ 200 g) are used. Actually, in this case the emissive neutron spectra, inclusive of both prompt fission and scattered neutrons, are measured. Only the high-energy part of the emissive spectrum with $E > E_{\rm n}$ corresponds exclusively to fission neutrons, evaporated from fission fragments. Measured PFNS data are fitted with simple analytical formulas (Maxwell or Watt), while average neutron energies are estimated using relevant fitting parameters of the assumed distribution. In other words, the deviation of real PFNS shape from the simple (Maxwell or Watt) formulas may lead to shifting of the average energy $\langle E \rangle$ of PFNS. Hence, it is rather difficult to define unambiguously the average energy $\langle E \rangle$ of the PFNS and its shape based on PFNS data, obtained with this method. The same happens in case of PFNS for spontaneous fission of ^{252}Cf, where a ~ 150 keV shift in $\langle E \rangle$ can appear, depending on the fitting energy intervals of fission neutrons. Average energy $\langle E \rangle$ data points for $E_{\rm n} \leqslant 6$ MeV [19–22], shown in fig. 1 with solid symbols, were obtained in the way described above. Some scattering of the $\langle E \rangle$ data points could be explained by the dependence on the fitting energy intervals of PFNS.

Another method is based on the application of multi-section fission chamber with layers of several grams of ^{238}U. This allows to distinguish fission neutrons against the background of elastic and inelastic scattered neutrons. Data points, plotted with open symbols in fig. 1, refer to the PFNS data, obtained with this method. However, some fission fragments may be lost due to nonzero registration threshold, the number of lost fission neutrons being dependent on the orientation of the chamber electrodes plane with respect to the neutron detector axis. This peculiarity may provoke systematic error in the measured neutron spectrum.

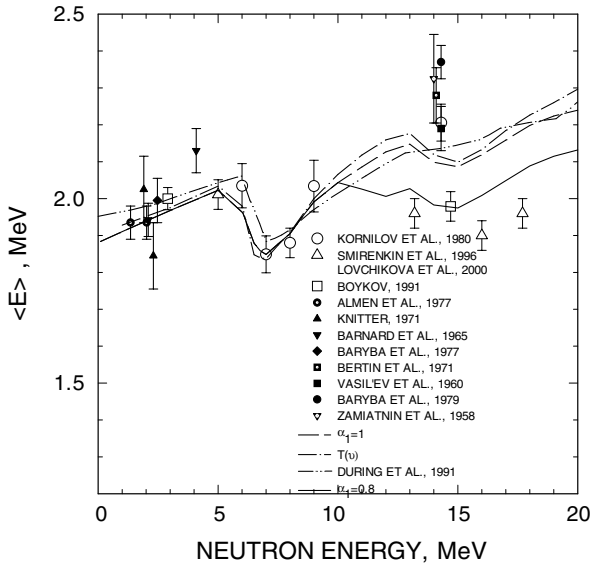

Fig. 1. Average energy $\langle E \rangle$ of PFNS. The solid line corresponds to $\alpha_1 = 0.8$, resembling CMS energy reduction; the dashed line corresponds to $\alpha_1 = 1$; the estimate based on eq. (8) is shown by a dash-dotted line; the dash-dot-dotted line is the calculation by During *et al.* [9].

Measured PFNS at $E_{\rm n} \sim 14$ MeV, reported in [5,6,23, 24] were assumed to be overloaded with pre-fission (n, $x$nf) neutrons. The data points [5,6,23,24] shown with solid symbols at $E_{\rm n} \sim 14$ MeV were measured with fission ionization chamber, except the data by Zamyatnin *et al.* [5]. It was assumed then that these neutrons have evaporation spectrum, average energy being rather low, with a cut-off energy around $E \sim 3$ MeV. The higher-energy part of the fission spectrum was fitted with Maxwell (Watt) distribution, PFNS average energy was calculated as $\langle E \rangle = 1.5T$ (Maxwell) or $\langle E \rangle = 1.5T + E_v$ (Watt), where T is the temperature parameter, while E_v is the fission fragment kinetic energy per nucleon. It is known now that a large fraction of pre-fission (n, nf) reaction neutrons is emitted via a pre-equilibrium process [1,2]. Consequently, the "temperature" parameter T, fitted over the high-energy tail of the neutron spectrum, to which these pre-fission (n, nf) neutrons contribute, would overestimate the value of the average PFNS energy $\langle E \rangle$ and distort the real post-fission neutron spectrum. For example, the average energy of the PFNS $\langle E \rangle = 2.087$ MeV is obtained for $E_{\rm n} = 14.7$ MeV. The temperature parameter T, when fitted over the neutron energy range $E \sim 3$–9 MeV gives $\langle E \rangle = 1.5T = 2.32$ MeV. The T value for PFNS data of

Table 1. $\nu_{\rm exp}$ estimated by PFNS integration and $\nu_{\rm p}$ measured and calculated data.

$E_{\rm n}$, MeV	References	$\nu_{\rm p}$ by Frehaut [25]	Present $\nu_{\rm p}$	$\nu_{\rm exp}$
6.0	Kornilov *et al.* [7]	3.214	3.212	3.34 ± 0.13
7.0	Kornilov *et al.* [7]	3.365	3.366	3.72 ± 0.14
8.0	Kornilov *et al.* [7]	3.517	3.515	3.79 ± 0.15
9.0	Kornilov *et al.* [7]	3.669	3.674	3.41 ± 0.15
14.3	Baryba *et al.* [6]	4.475	4.495	5.09 ± 0.15
14.7	Lovchikova *et al.* [4]	4.536	4.550	4.25 ± 0.10
16.0	Lovchikova *et al.* [4]	4.728	4.713	4.48 ± 0.13
17.7	Lovchikova *et al.* [4]	4.920	4.937	4.52 ± 0.14

Baryba *et al.* [6], shown in fig. 1 with solid circle, should be considered to be too high.

PFNS above emissive fission threshold are represented with data of two sets of experiments. The first one, by Baryba *et al.* [6] and Kornilov *et al.* [7] and the second one, by Boykov *et al.* [1,2], Smirenkin *et al.* [3] and Lovchikova *et al.* [4]. In experiments of both sets neutrons were registered in coincidence with fission events, a multi-section fission chamber was used to separate fission events, while a time-of-flight technique was employed for the neutron spectra measurements. In both measurements PFNS for the ^{238}U(n, f) reaction were measured relative to those of ^{252}Cf. Time resolutions (2–3 ns) and flight paths (~ 2 m) in both sets of experiments were similar. However, estimates of the average energy of PFNS, measured in these experiments are rather different (see fig. 1). This may be explained as follows.

In the experiment of the first set by Baryba *et al.* [6], the fission chamber efficiency was $\sim$ 70–75% at $E_{\rm n} \sim$ 14.3 MeV and $\sim$ 80–85% for $E_{\rm n} \sim$ 6–9 MeV. In the experiment of the second set by Lovchikova *et al.* [4], the efficiency was still higher. In the measurement by Baryba *et al.* [6], the electrodes with layers of ^{238}U were oriented in such a way that the neutron detector axis was perpendicular to the chamber electrodes plane. Henceforth, fission fragments, moving along the electrodes plane might be lost. The prompt fission neutron spectra for fixed fission fragment directions are plotted in fig. 2. Due to the kinematics effect, the total amount of neutrons and their average energy are much less for the 90°-direction, than for the 0°-direction. As a result, in the set-up of the experiment by Baryba *et al.* [6] the total amount of lost neutrons, would be less as compared with the total number of fission fragments below the registration threshold. Lost neutrons have smaller energy as compared with the average value $\langle E \rangle$. Because of this fact, a higher average fission neutron energy $\langle E \rangle$ is expected in the experiment by Baryba *et al.* [6]. As a consequence, due to fission fragment discriminations the direct correlation should be observed, *i.e.*, a high average energy of measured spectrum $\langle E \rangle$ should be accompanied by a higher neutron multiplicity value $\nu_{\rm exp}$. Values of $\nu_{\rm exp}$, estimated from measured PFNS data, as well as calculated $\nu_{\rm p}$ data are summarized in table 1. Note the rather strong difference of $\nu_{\rm exp}$ and $\nu_{\rm p}$ ($\sim 10\%$), it is much higher than assigned errors for $E_{\rm n} \sim 14.3$ MeV data point [6].

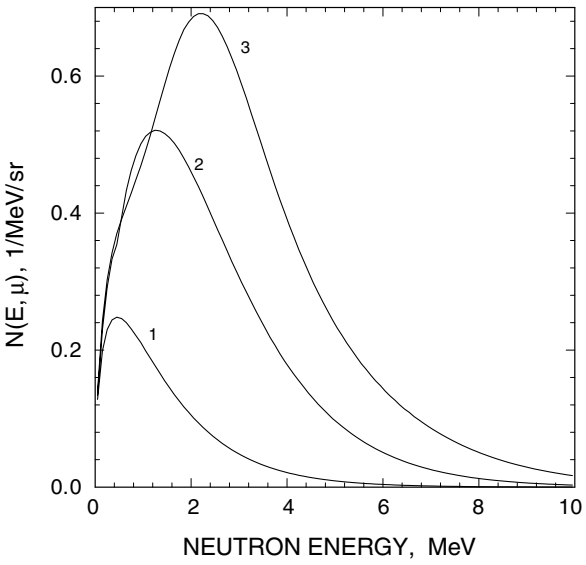

Fig. 2. Fission neutron spectra *versus* energy and cosine μ to the fragment direction in the laboratory system; 1: spectrum at 90°, 2: 0° for the heavy fragment and 3: for the light fragment.

In the experiment of the second set by Lovchikova *et al.* [4] a different orientation of the fission chamber electrodes relative to the neutron detector axis was employed. In addition, some amount of ^{252}Cf was incorporated into one section of the fission chamber as an admixture to the uranium layer. It allowed to reduce the influence of the fragment discrimination threshold on measured PFNS and neutron multiplicity $\nu_{\rm exp}$. However, it seems that the influence of the fission chamber efficiency was reduced, but still not eliminated; in other words, the differences of $\nu_{\rm exp}$ are still noticeable. Values of $\nu_{\rm exp}$ are lower than measured and evaluated (5th column) by Frehaut [25] (see table 1). In all cases, shown in table 1, the values of $\nu_{\rm exp}$ by Baryba *et al.* [6] (except $E_{\rm n} \sim 9$ MeV data point) are higher than the present calculated values of $\nu_{\rm p}$, while values of $\nu_{\rm exp}$ by Lovchikova *et al.* [4] are lower. This peculiarity shows that experimental data of these measurements also may contain a systematic error.

In the experiments of the first set, *i.e.*, by Baryba *et al.* [6] and Kornilov *et al.* [7], neutrons were detected in coincidence with fission events, but there was no timing of events. The spectra were measured in a "pulsed

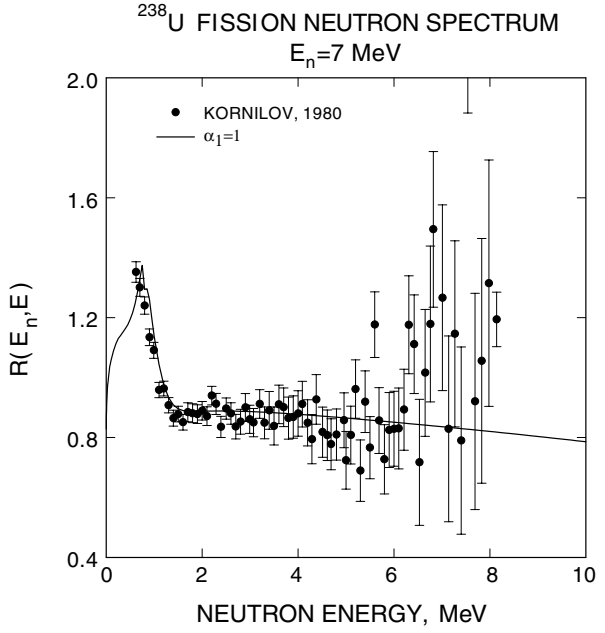

Fig. 3. Measured and calculated PFNS at $E_{\rm n} = 7\,{\rm MeV}$ relative to Maxwell PFNS with the same average energy $\langle E\rangle = 2.024\,{\rm MeV}$.

mode" of the accelerator. Consequently, the spectrum of "background" neutrons was time dependent and the "effect/background" ratio was poor at higher neutron energies. This explains neutron excess in PFNS above $E \sim 6\,{\rm MeV}$ (see fig. 3 for $E_{\rm n} = 7\,{\rm MeV}$). Henceforth, we suppose that data of the experiments of the second set, *i.e.*, by Boykov *et al.* [1,2], Smirenkin *et al.* [3] and Lovchikova *et al.* [4], define more realistic level of PFNS average energies $\langle E\rangle$.

Available PFNS data by Boykov *et al.* [1,2], Smirenkin *et al.* [3], Lovchikova *et al.* [4], Svirin *et al.* [10], Baryba *et al.* [6], Kornilov *et al.* [7] and Kornilov [8], are, with minor exceptions, relative data without absolute normalization. When absolute normalization is provided, it has a high systematic error. To compare measured and calculated data, we normalized the PFNS experimental data by least-squares fit as

$$F(C) = \sum_i \left(N_i - CS_i\right)^2 \cdot \omega_i, \quad \omega_i = \frac{1}{\delta N_i^2}\,; \qquad (1)$$

here S_i is the calculated value at energy E_i, ω_i is the weight of the i-th measured data point, δN_i is the absolute error of the experimental value N_i. The value of the coefficient C was estimated by solving the equation ${\rm d}F/{\rm d}C = 0$, which gives

$$C = \frac{\sum\limits_i S_i \cdot N_i \cdot \omega_i}{\sum\limits_i S_i^2 \cdot \omega_i}\,. \qquad (2)$$

The data presented by open symbols in fig. 1 were estimated by numerical integration of the experimental spectra. The lowest and highest parts of the spectra were fitted by a simple Maxwellian and its parameters were applied for the relevant extrapolations.

3 Model for PFNS calculation

In the energy range of non-emissive or first-chance fission, PFNS were calculated as described elsewhere (see Kornilov *et al.* [26]). It was shown that PFNS can be described as a sum of two Watt distributions:

$$S_i\left(E, E_{\rm n}\right) = 0.5 \sum_{j=1}^{2} W_i\left(E, E_{\rm n}, T_{ij}\left(E_{\rm n}\right), \alpha\right), \qquad (3)$$

$$W_i\left(E, E_{\rm n}, T_{ij}\left(E_{\rm n}\right), \alpha\right) = M\left(E, T_{ij}\right) \times \exp\left(-\frac{\tilde{E}_{vij}}{T_{ij}}\right) \frac{{\rm sh}\left(\sqrt{b_{ij}E}\right)}{\sqrt{b_{ij}E}}\,, \qquad (4)$$

$$M\left(E, T_{ij}\right) = \frac{2\sqrt{E}}{\sqrt{\pi}T_{ij}^{3/2}} \exp\left(-\frac{E}{T_{ij}}\right), \qquad (5)$$

$$b_{ij} = \frac{4\tilde{E}_{vij}}{T_{ij}^2}, \quad T_{ij} = k_{ij}\sqrt{E_i^*} = k_{ij}\sqrt{E_r - TKE_i + U_i}. \qquad (6)$$

T_{ij} is the temperature parameter for light (1) and heavy (2) fragments ($j = 1, 2$) of the i-th nucleus, α is the ratio of the total kinetic energy (TKE_i) at the moment of neutron emission to the appropriate TKE_i value for the i-th fissioning nucleus in the full acceleration limit. In Watt's equation (eq. (4)) the CMS energy per nucleon is reduced as $\tilde{E}_{\nu ij} = \alpha \cdot E_{\nu ij}$, *i.e.*, $\tilde{E}_{v1i} = \frac{A_{2i}}{A_{1i} \cdot A_i} \cdot \alpha \cdot TKE_i$, $\tilde{E}_{v2i} = \frac{A_{1i}}{A_{2i} \cdot A_i} \cdot \alpha \cdot TKE_i$. Experimental PFNS data were fitted assuming that α is a free parameter. The ratio of "temperatures" for light and heavy fragments $T_{i1}/T_{i2} = 1.248$ is the second semi-empirical fitting parameter, which was assumed to be independent of the nucleon composition of the actinide fissioning nucleus. This approach allows to reach better agreement with experimental data on PFNS for non-emissive neutron-induced fission. Figure 4 shows the $^{238}{\rm U(n,f)}$ reaction PFNS for $E_{\rm n} = 5\,{\rm MeV}$, the calculated curve is compatible with experimental data in the energy range of $E \sim 0.5$–$12\,{\rm MeV}$. We assume that eqs. (3), (4), (5) and (6) approximate post-fission neutron spectra for incident neutron energies below the emissive fission threshold.

Above the emissive fission threshold, *i.e.* in the incident neutron energy range $E_{\rm n} \gtrsim 6\,{\rm MeV}$, PFNS are described as a superposition of pre-fission (n, $x$nf) reaction neutrons and prompt fission neutrons, emitted from $^{238+1-i}{\rm U}$ nuclides after emission of i pre-fission neutrons:

$$\begin{aligned} S\left(E, E_{\rm n}\right) = \nu^{-1}\left(E_{\rm n}\right)\Big(&\nu_0\left(E_{\rm n}\right) \cdot \beta_0\left(E_{\rm n}\right) \cdot S_0\left(E, E_{\rm n}\right) \\ &+\nu_1\left(E_{\rm n}\right) \cdot \beta_1\left(E_{\rm n}\right) \cdot S_1\left(E, E_{\rm n}\right) + \beta_1\left(E_{\rm n}\right) \cdot P_{11}\left(E, E_{\rm n}\right) \\ &+\nu_2\left(E_{\rm n}\right) \cdot \beta_2\left(E_{\rm n}\right) \cdot S_2\left(E, E_{\rm n}\right) \\ &+\beta_2\left(E_{\rm n}\right) \cdot \left[P_{21}\left(E, E_{\rm n}\right) + P_{22}\left(E, E_{\rm n}\right)\right] + \cdots\Big), \end{aligned} \qquad (7)$$

$$\int P_{ij}\left(E, E_{\rm n}\right){\rm d}E = 1,$$

$$\nu\left(E_{\rm n}\right) = \sum_{i=0} \left[\left(\nu_i\left(E_{\rm n}\right) + i\right) \cdot \beta_i\left(E_{\rm n}\right)\right]; \qquad (8)$$

the subscript $i = 0, 1, 2\ldots$ denotes multiple-chance fission of $^{239}{\rm U}$, $^{238}{\rm U}$ and $^{237}{\rm U}$ after emission of i pre-fission

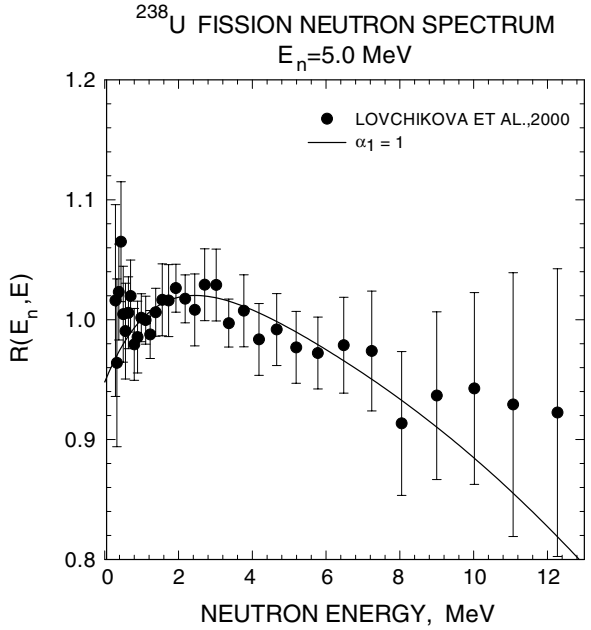

Fig. 4. Measured and calculated PFNS at $E_{\rm n} = 5\,$MeV relative to Maxwell PFNS with the same average energy $\langle E\rangle = 2.023\,$MeV.

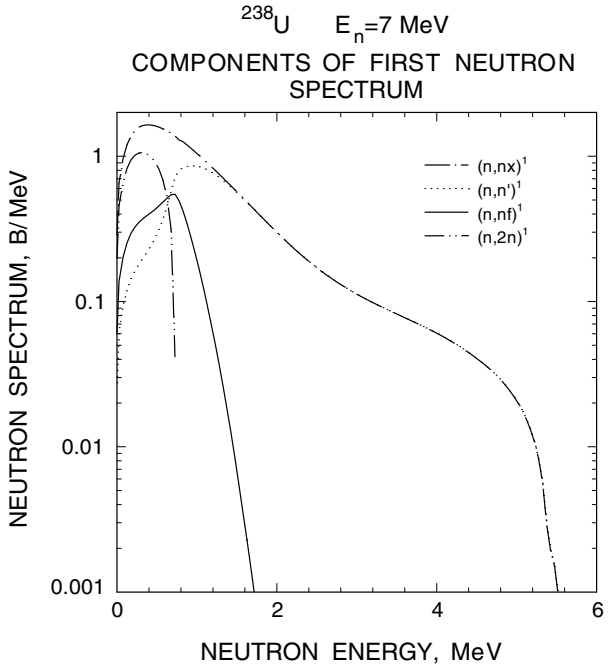

Fig. 5. Partial neutron spectra at $E_{\rm n} = 7\,$MeV.

(n, $x$nf) neutrons, $\beta_i(E_{\rm n})$ is the contribution of the i-th chance fission reaction to the observed fission cross-section, $\nu_i(E_{\rm n})$ is the number of prompt fission neutrons for ^{239}U, ^{238}U and ^{237}U fissioning nuclides, which have spectra $S_i(E, E_{\rm n})$ (see eq. (3)), $P_{ij}(E, E_{\rm n})$ is the spectrum of the j-th pre-fission neutron for the i-th chance fission. To calculate the observed PFNS, the $\nu_i(E_{\rm n})$, $\beta_i(E_{\rm n})$ and T_{ij} values should be estimated.

The excitation energy U_i of the nucleus $A_i = A+1-i$ after the emission of i neutrons was calculated as

$$U_i = E_{\rm n} + B_{\rm n} - \sum_{j\le i} \left(\langle E_{ij}\rangle + B_j\right); \qquad (9)$$

here B_j is the neutron binding energy for the relevant residual nuclide. We estimated the excitation energy of fission fragments as $E_i^* = E_{\rm r} + U_i - TKE$ and calculated the $T_{ij}(E_{\rm n})$ *versus* excitation energy for each fissioning nucleus.

The systematics by Malinovskij [27] was used to estimate the prompt fission neutron number $\nu_i(E_{\rm n})$ below the emissive fission threshold. In this systematics $\nu_i(E_{\rm n})$ was estimated for spontaneous and neutron-induced fission for a number of actinide nuclei. We assumed that the excitation energy U_i is brought to the A_i nucleus with the reaction: n+A_{i-1} → fission. The incident neutron energy $E_{\rm n}$ in this reaction equals $U_i - B_{i-1}$. The $\nu_i(E_{\rm n})$ for the relevant U fissioning nuclides ^{239}U, ^{238}U and ^{237}U were calculated. The total numbers of prompt fission neutrons $\nu(E_{\rm n})$ were calculated with eq. (8) and are shown in table 1.

Figures 3 and 4 show that the present model correctly describes the PFNS data either for $E_{\rm n} = 7\,$MeV and $E_{\rm n} = 5\,$MeV. Similar conclusion can be made for measured PFNS data for $E_{\rm n}$ up to ∼ 9 MeV, *i.e.* the PFNS average-energy $\langle E\rangle$ data trend also would be reproduced. The calculated curve reproduces the minimum of the average neutron energy of PFNS at $E_{\rm n} \sim 7\,$MeV (see fig. 1). The pre-fission (n, nf)-reaction spectra contribution allows to reproduce measured prompt fission neutron spectrum in fig. 3. Partial components of the first neutron spectrum for $E_{\rm n} = 7\,$MeV are shown in fig. 5. The pre-fission neutron spectrum of the (n, nf) reaction is defined by competition with the first neutron spectrum of the (n, 2n) and (n, nγ) reactions. The prompt fission spectrum at $E_{\rm n} \lesssim E_{\rm th} \sim E_{\rm n} - B_{\rm f} \sim 2\,$MeV demonstrates the contribution of (n, nf) pre-saddle neutrons.

3.1 Extrapolation above the (n, 2nf) threshold energy

The model described in the previous paragraph could not reproduce the PFNS data shape at incident neutron energies $E_{\rm n} \gtrsim 13\,$MeV, *i.e.*, above the (n, 2nf) reaction threshold, see dashed curve in fig. 6 showing calculated PFNS for $E_{\rm n} \sim 16\,$MeV. Discrepancies of the calculated and measured PFNS data of the same kind are observed for $E_{\rm n} \sim$ 13.2, 14.7 and 17.7 MeV [17]. However, the increase of cut-off energy $E_{\rm th} \sim E_{\rm n} - B_{\rm f}$ of the (n, nf) reaction neutron spectra with the increase of the excitation energy of the fissioning nucleus is reproduced, *i.e.*, $E_{\rm th} \sim 9\,$MeV for $E_{\rm n} \sim 16\,$MeV, while $E_{\rm th} \sim 11\,$MeV for $E_{\rm n} \sim 17.7\,$MeV. A step-like irregularity around $E \sim 3\,$MeV for $E_{\rm n} \sim 16\,$MeV (see fig. 6) and $E \sim 5\,$MeV for $E_{\rm n} \sim 17.7\,$MeV (see fig. 7) could be correlated with the first neutron spectrum of the ^{238}U(n, 2nf) reaction. First neutron spectra of the (n, nf) and (n, 2nf) reactions for $E_{\rm n} \sim 16\,$MeV and $E_{\rm n} \sim 17.7\,$MeV are shown in fig. 8.

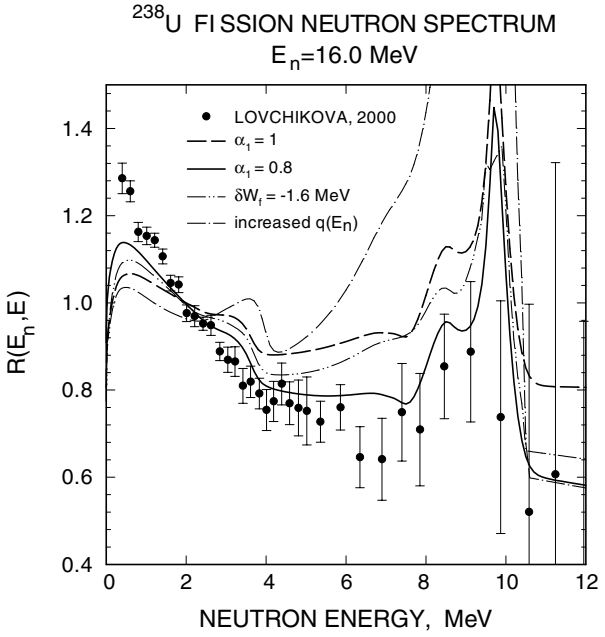

Fig. 6. Measured and calculated PFNS at $E_{\rm n} = 16\,{\rm MeV}$ relative to Maxwell PFNS with the same average energy $\langle E\rangle = 2.191\,{\rm MeV}$. The solid line corresponds to $\alpha_1 = 0.8$, resembling the CMS energy reduction; the dashed line corresponds to $\alpha_1 = 1$; the dash-dotted line corresponds to the deacreased fission probability of ^{239}U (negative outer saddle shell correction); the dash-dot-dotted line corresponds to the increased pre-equilibrium emission of first neutron.

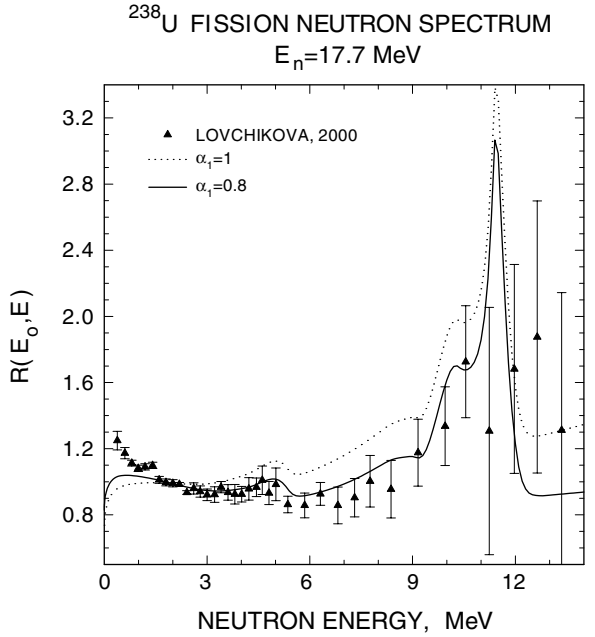

Fig. 7. Measured and calculated ^{238}U PFNS at $E_{\rm n} = 17.7\,{\rm MeV}$ relative to Maxwell PFNS with average energy $\langle E\rangle = 2.0878\,{\rm MeV}$. The solid line corresponds to $\alpha_1 = 0.8$, resembling the CMS energy reduction; the dotted line corresponds to $\alpha_1 = 1$.

Other partial neutron spectra of $^{238}{\rm U}({\rm n}, x{\rm nf})$ reactions have roughly evaporative shape.

In principle, the discrepancy of calculated PFNS (see dashed line in fig. 6) and measured data could be attributed to the erroneous estimate of the main temperature parameters T_{ij} for the post-fission neutron spectrum calculation with eq. (6). To validate the T_{ij} temperature parameter values, we calculated the average PFNS energy, using the same $\nu_i(E_{\rm n})$, $\beta_i(E_{\rm n})$ and $\langle E_{ij}\rangle$ functions, as earlier, while average energies for post-fission neutrons were calculated as recommended in [7,8]:

$$\langle E_i\rangle = 1.5T_i = 1.5 \times \left(a + b\sqrt{\nu_i + 1}\right),$$
$$a = 0.41, \qquad b = 0.47. \tag{10}$$

The relevant dependence of the average neutron energy $\langle E\rangle$ *versus* incident neutron energy $E_{\rm n}$ is shown in fig. 1 by the dashed line. The estimate of $\langle E\rangle$ by During *et al.* [9], obtained taking into account multiple-chance fission, is also shown in fig. 1 by the dash-dot-dotted line. Theoretical models, the present and that by During *et al.* [9], predict roughly the same increasing trend at higher $E_{\rm n}$ values. Particular features of the models are: a) "temperature" parameter $T \sim \sqrt{E_{\rm n}}$, b) coefficients k_{ij} and a, b in eqs. (6) and (10) were adjusted to fit the measured PFNS data for $E_{\rm n} \lesssim 6\,{\rm MeV}$.

The comparison of calculated PFNS with measured data shows that the present model describes the measured PFNS at $E_{\rm n} \lesssim 9\,{\rm MeV}$ [17], but fails at higher $E_{\rm n}$ energies,

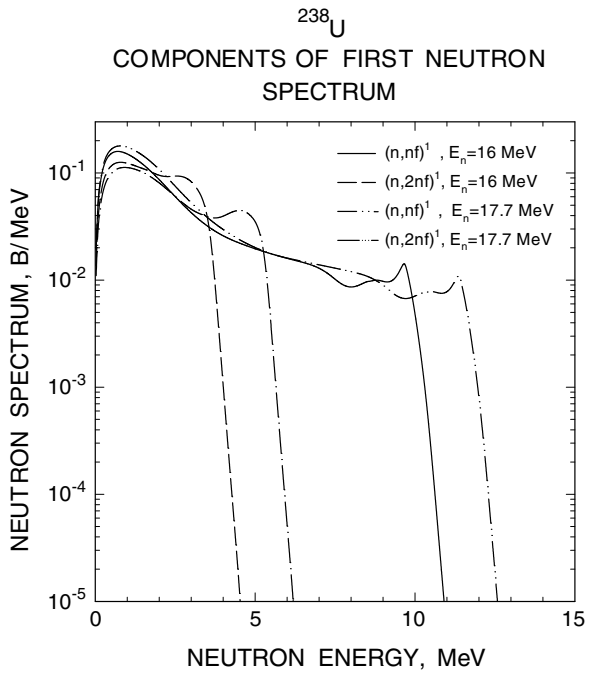

Fig. 8. First neutron spectra of $^{238}{\rm U}({\rm n}, {\rm nf})$ and $^{238}{\rm U}({\rm n}, 2{\rm nf})$ reactions at $E_{\rm n} = 16\,{\rm MeV}$ and $E_{\rm n} = 17.7\,{\rm MeV}$.

actually above the $^{238}{\rm U}({\rm n}, 2{\rm nf})$ reaction threshold. In the following sections we will discuss possible ways to mitigate this discrepancy, *i.e.* assumption of neutron emission during fission fragment acceleration, multiple-chance fission contribution variation and addition of an extra neutron source.

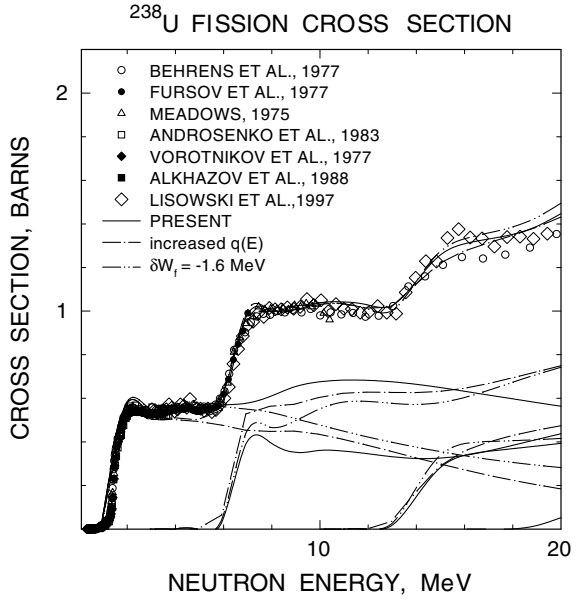

Fig. 9. ^{238}U(n, F) fission cross-section; the solid line represents the present results; the dash-dotted line corresponds to the deacreased fission probability of ^{239}U (negative outer saddle shell correction); the dash-dot-dotted line corresponds to the increased pre-equilibrium emission of first neutron.

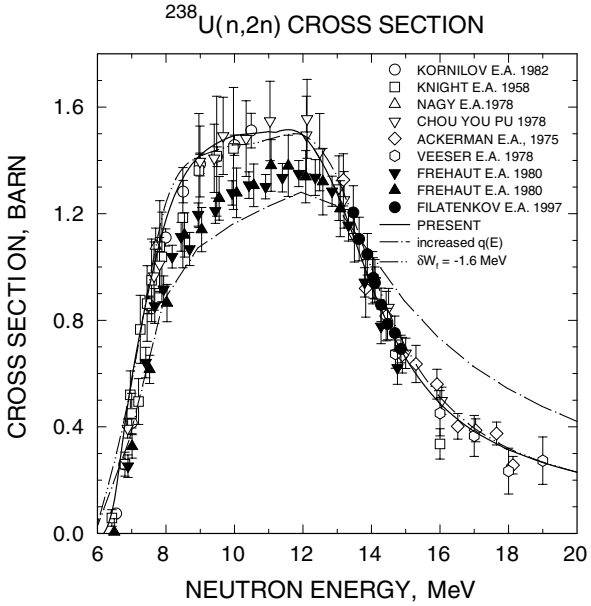

Fig. 10. ^{238}U(n, 2n) reaction cross-section; the solid line represents the present results; the dash-dotted line corresponds to the deacreased fission probability of ^{239}U (negative outer saddle shell correction); the dash-dot-dotted line corresponds to the increased pre-equilibrium emission of first neutron.

3.2 Neutron emission during fragment acceleration

It was proposed by Eismont [28] that for excitations higher than $\sim$ 20 MeV prompt fission neutrons could be emitted from the fragments before their full acceleration. That means that for $E_{\rm n} \sim 14$ MeV or higher, the neutron emission time might be comparable with the ^{238}U(n, f) fission fragments acceleration time of $\sim 10^{-20}$ s; in other words, some neutrons could be emitted during fragments acceleration. Consequently, the center-of-mass system energy and average neutron energy in the Laboratory System would be reduced [29]. We assume that the CMS energy per one nucleon $E_{\nu ij}$ could be further reduced (see eqs. (4)-(6)) as

$$\widetilde{E}_{\nu ij} = \alpha_1 \cdot \alpha \cdot E_{\nu ij}, \qquad (11)$$

here $\alpha_1 = 1$ for $E_{\rm n} < 10$ MeV and $\alpha_1 = 0.8$ for $E_{\rm n} > 12$ MeV, it is linearly interpolated for $10 \leq E_{\rm n} \leq 12$ MeV. This correction was made for the ^{238}U(n, f), ^{238}U(n, nf) and ^{238}U(n, 2nf) multiple-chance fission reactions. The relevant calculated $\langle E \rangle$ and PFNS are shown in figs. 1 and 6 by solid lines. This additional lowering of average energy of PFNS due to the reduced fission fragment velocity at the moment of neutron emission removes the major discrepancy between calculated spectra and measured data. This hypothesis roughly describes also the reduction of the average energy of PFNS $\langle E \rangle$.

3.3 Multiple-chance fission

The contributions of the i-th multiple-chance fission reactions to the observed fission cross-section $\beta_i(E_{\rm n})$ and pre-fission neutron spectra $P_{ij}(E, E_{\rm n})$, *i.e.*, spectra of the j-th pre-fission neutrons for the i-th chance fission, were calculated in a Hauser-Feshbach statistical-model simultaneously with the ^{238}U(n, F) [30–35] (see fig. 9) ^{238}U(n, 2n) [36–44] (see fig. 10) and ^{238}U(n, 3n) [40,42] (see fig. 11) reaction cross-sections [17,18]. The pre-equilibrium first-neutron emission was taken into account, then average neutron energies $\langle E_{ij} \rangle$ were estimated. Contributions of the ^{238}U(n, f), ^{238}U(n, nf) and ^{238}U(n, 2nf) fission reactions to the observed ^{238}U(n, F) fission cross-section are shown in fig. 9. There are different estimates of multiple-chance fission contributions to the observed fission cross-section of ^{238}U [10,15,16], in our approach first-chance non-emissive fission cross-section of the ^{238}U(n, f) reaction is a weak function of the incident neutron energy [17,18]. Contributions of second-chance ^{238}U(n, nf) and third-chance ^{238}U(n, 2nf) fission reaction are defined by ^{237}U(n, f) and ^{236}U(n, f) non-emissive fission cross-sections description in the first "plateau" region, respectively. We argue that other estimates of multiple-chance fission contributions [16] would deteriorate the consistent description of ^{238}U(n, F), ^{238}U(n, 2n) and ^{238}U(n, 3n) or non-emissive ^{237}U(n, f) and ^{236}U(n, f) reaction cross-sections, though they could improve the description of the measured PFNS data.

Indeed, pre-fission (n, $x$nf) neutron emission lowers the excitation energy of residual nuclei. Reducing the contribution of non-emissive first-chance fission, *i.e.* ^{238}U(n, f) reaction, and increasing the contribution of multiple-chance fission, *i.e.*, ^{238}U(n, nf) and ^{238}U(n, 2nf) reactions, we could reduce the average energy of PFNS down to the level predicted by PFNS data by Boykov *et al.* [1],

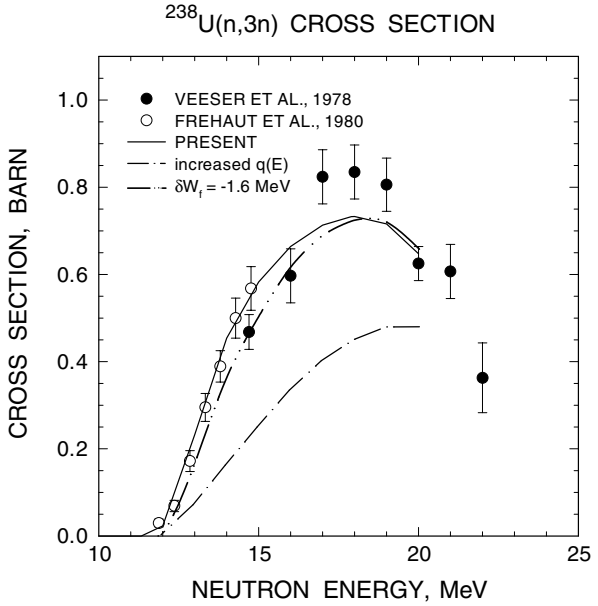

Fig. 11. ^{238}U(n, 3n) reaction cross-section; solid line represents the present results; the dash-dot-dotted line corresponds to the deacreased fission probability of ^{239}U (negative outer saddle shell correction); the dash-dotted line corresponds to increased pre-equilibrium emission of first neutron.

Smirenkin *et al.* [3] and Lovchikova *et al.* [4]. Redistribution of multiple-chance fission contributions to the observed PFNS may mitigate the discrepancy of calculated PFNS with measured data. There are two options to reduce non-emissive first-chance fission cross-section [18]. Since the behavior of the first-chance fission cross-section $\sigma_{\rm f1}$ is obviously related to the energy dependence of the first-chance fission probability of the ^{239}U nuclide $P_{\rm f1}$,

$$\sigma_{\rm f1} = \sigma_{\rm r}\big(1 - q\big(E_{\rm n}\big)\big)P_{\rm f1}, \qquad (12)$$

its contribution to the observed fission cross-section could be lowered by increasing the contribution of first neutron pre-equilibrium emission $q(E_{\rm n})$, or decreasing the first-chance fission probability $P_{\rm f1}$. The first-chance fission probability $P_{\rm f1}$ depends only on the level density parameters of the fissioning ^{239}U and residual ^{238}U nuclides. Actually, it depends on the ratio of shell correction values at the outer saddle deformations of the double-humped fission barrier $\delta W_{\rm f}$ and $\delta W_{\rm n}$. Different theoretical estimates of the shell corrections as well as of the fission barriers vary by 1–2 MeV. The same is true for the experimental shell corrections, which are obtained with a smooth component of potential energy calculated according to the liquid-drop or droplet model. However, the isotopic changes of $\delta W_{\rm f}$ and $\delta W_{\rm n}$ [45] are such that $P_{\rm f1}$ viewed as a function of the difference $(\delta W_{\rm f} - \delta W_{\rm n})$ is virtually independent of the choice of smooth component of potential energy. Therefore, we shall consider the adopted $\delta W_{\rm f} = 0.6$ MeV estimate to be effective, provided that $\delta W_{\rm n}$ values are obtained with the liquid-drop model. The trend of the first-chance fission cross-section $\sigma_{\rm f1}$ shown in fig. 9 (solid line) could be treated as a manifestation of the shell effects in the first-chance fission probability. This estimate of $\sigma_{\rm f1}$ corresponds to the consistent fit of the (n, 2n) and (n, 3n) reaction cross-section data for ^{238}U. The increasing contribution of the pre-equilibrium neutron to the spectrum of the first neutron would severely distort the ^{238}U(n, 2n) reaction cross-section, it would be severely overestimated at $E_{\rm n} \gtrsim 13$ MeV (see fig. 10), while the ^{238}U(n, 3n) reaction cross-section would be underestimated (see fig. 11). The influence of the increasing contribution of the pre-equilibrium neutron is shown by the dash-dotted curve in fig. 6, it seems to be incompatible with the measured PFNS data trend.

The first-chance fission probability $P_{\rm f1}$ also could be decreased assuming $\delta W_{\rm f} = -1.6$ MeV. Nonetheless, the total fission cross-section could be kept unaffected, the decreased contribution of the first-chance fission cross-section $\sigma_{\rm f1}$ could be compensated by increasing the fission probabilities of the ^{238}U and ^{237}U nuclides well above the level, predicted by the ^{237}U(n, f) and ^{236}U(n, f) cross-sections (see fig. 9). Cross-sections of ^{238}U(n, 2n) and ^{238}U(n, 3n) reactions in this case are not much different from the present estimate. The influence of the increasing contribution of multiple-chance fission reactions is shown by the dash-dot-dotted curve in fig. 6. In that case the contribution of soft neutrons somewhat increases, but at higher fission neutron energies the calculated curve is still incompatible with the measured PFNS data trend. Note that the contribution of second-chance fission keeps increasing at $E_{\rm n} \gtrsim 14$ MeV in all cases considered, while Kawano *et al.* [16] predict its sharp lowering with subsequent strong increase of the third-chance fission contribution. The decreasing trend of the non-emissive fission cross-section of ^{238}U(n, f), as well as the high contributions of second-chance ^{238}U(n, nf) and third-chance ^{238}U(n, 2nf) to the observed fission cross-section of ^{238}U, predicted by Kawano *et al.* [16] seem to be unjustified, since it deteriorates the consistent description of the ^{238}U(n, F) and ^{238}U(n, xn) reaction cross-sections (see figs. 9, 10 and 11).

3.4 Additional neutron source

PFNS data for $E_{\rm n} \gtrsim 9$ MeV could be fitted introducing an additional source of soft neutrons, emitted from non-accelerated fragments, as was proposed by Svirin *et al.* [10]. They suggested that PFNS can be represented as

$$S_u\big(E, E_{\rm n}\big) = \eta \cdot \varphi_u(E) + (1 - \eta) \cdot S\big(E, E_{\rm n}\big); \qquad (13)$$

here $S(E, E_{\rm n})$ is the spectrum of PFNS from fission fragments, defined by eq. (3), parameters are the same as those used without additional neutron source. The spectrum $\varphi_u(E)$ of this neutron source is represented as

$$\varphi_u(E) = \frac{E}{T_u^2} \exp\left(-\frac{E}{T_u}\right). \qquad (14)$$

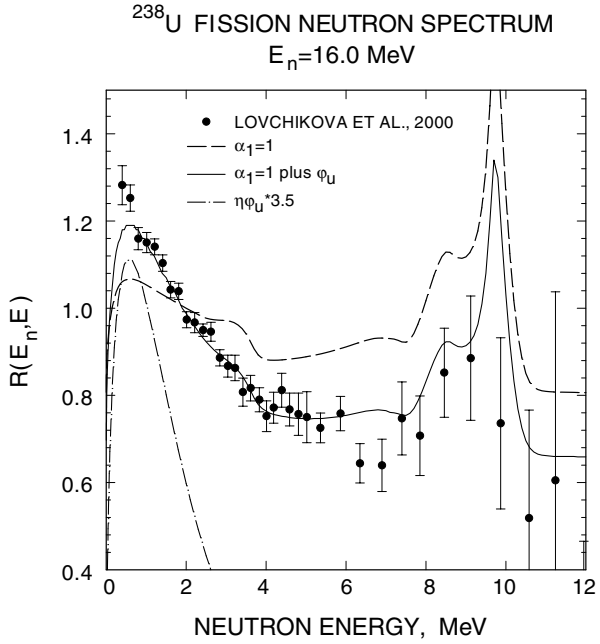

Fig. 12. Measured and calculated PFNS relative to Maxwell PFNS with the same average energy $\langle E\rangle = 2.191\,\mathrm{MeV}$. The solid line corresponds to calculations with an additional neutron source $\varphi_u(E)$; the dash-dotted line shows the contribution of the additional neutron source $\eta\varphi_u(E)$; the dashed line corresponds to the calculations with eqs. (3)-(8) with $\alpha_1 = 1$.

The calculated spectrum with adjusted parameters $\eta = 0.18$, $T_u = 0.64\,\mathrm{MeV}$ ($\nu_u = \eta\nu = 0.86$ neutrons/fission, $\langle E\rangle = 1.28\,\mathrm{MeV}$) is shown in fig. 12 by a solid line. The spectrum of these neutrons $\eta{\cdot}\varphi_u(E)$, multiplied by a factor of 3.5 for convenience, is shown with a dash-dotted line.

Inclusion of this additional neutron source also decreases the discrepancy of calculated PFNS with measured data, but the properties of this neutron source look rather strange. Svirin *et al.* [10] found that the yield of these neutrons is $\sim$ 0.5 neutrons/fission and their average energies $\langle E\rangle \sim 0.5$–$0.7\,\mathrm{MeV}$. They assumed that these soft neutrons are emitted from separated fragments staying at rest. Then the neutron emission time should be rather short, because emission should occur before full acceleration. The energies of emitted neutrons should be low, which corresponds to low excitation of the fragments. Svirin *et al.* [10] argue that the excitation energy for each of the fragments is $\sim$ 5–6 MeV. A compound nucleus at an excitation energy of $\sim$ 5–6 MeV has a neutron emission lifetime of 10^{-18}–10^{-17} s. A similar neutron emission time was obtained by Moretto [46]. It was shown by Knitter *et al.* [47] and Kornilov *et al.* [48] that the total kinetic energy reaches $\sim$ 90% of its maximum value within $\sim 10^{-20}$ s. That means neutrons could not be emitted from fragments with low excitations before acceleration. Hence, if an additional neutrons source exists, it should be of rather exotic nature, *i.e.*, its strength should increase with incident neutron energy.

4 Conclusion

We investigated several options to describe ^{238}U(n, f) PFNS data in a multiple-chance fission excitation energy range. Namely, neutron emission from fission fragments before full acceleration, increase of emissive fission chances contributions and introduction of an additional neutron source. The latter option, incorporation of an additional neutron source, allows to reproduce measured PFNS data, but its properties look rather contradictory. Variation of emissive fission contributions to the observed fission cross-section, *i.e.*, the increase of the ^{238}U(n, nf) and especially ^{238}U(n, 2nf) contributions to the fission observables, somewhat helps to decrease the discrepancies of measured and calculated PFNS. However, strong variation of the fission chance structure, which might describe the PFNS data trend, is at odds with a self-consistent description of the ^{238}U(n, f) and ^{238}U(n, xn) reaction cross-sections and fission probability estimates of the ^{238}U and ^{237}U nuclides.

At present, the absolute value of the total kinetic energy at the moment of neutron emission is lower than values predicted from excitation energy of the fragments and acceleration time [48]. However, modeling of neutron emission from fission fragments before full acceleration allows to describe PFNS data for incident neutron energies up to $\sim$ 18 MeV, for a fission neutron energy range $E \gtrsim 1.5\,\mathrm{MeV}$. The increase of the cut-off energy $E_{\mathrm{th}} \sim E_{\mathrm{n}} - B_{\mathrm{f}}$ of the (n, nf) reaction neutron spectra with excitation energy of the fissioning nucleus is reproduced for $E_{\mathrm{n}} = 6$–$18\,\mathrm{MeV}$. Step-like irregularities around $E \sim 3\,\mathrm{MeV}$ for $E_{\mathrm{n}} \sim 16\,\mathrm{MeV}$ and $E \sim 5\,\mathrm{MeV}$ for $E_{\mathrm{n}} \sim 17.7\,\mathrm{MeV}$ could be correlated with the first neutron spectrum of the ^{238}U(n, 2nf) reaction. The detailed analysis of neutron emission during fragment acceleration will need accurate data on the angular distribution of prompt fission neutrons. Some excess of soft neutrons with $E \lesssim 0.5\,\mathrm{MeV}$ could be attributed to neutrons, emitted during transition from saddle to scission (for details, see a review by Hilscher and Rossner [14]).

Summarizing, we argue that correct estimate of the pre-fission (n, $x$nf) reaction spectra, alongside with simple modelling of spectra of neutrons, emitted from fission fragments, provides a versatile theoretical tool for the analysis of measured PFNS data for target nuclides with various fissilities, *i.e.*, ^{232}Th, ^{235}U and ^{237}Np.

This Research was supported by International Science and Technology Center under the Project Agreement B-404. The Funding Party for the Project is Japan.

References

1. G.S. Boykov, V.D. Dmitriev, G.A. Kudyaev *et al.*, Yad. Fyz. **53**, 628 (1991).
2. G.S. Boykov, V.D. Dmitriev, M.I. Svirin *et al.*, Phys. At. Nucl. **57**, 2047 (1994).
3. G.N. Smirenkin, G.N. Lovchikova, A.M. Trufanov *et al.*, Yad. Fyz. **59**, 1934 (1996).

4. G.N. Lovchikova, A.M. Trufanov, M.I. Svirin *et al.*, in *Proceedings of the XIV International Workshop on Nuclear Fission Physics*, *Obninsk, October, 12-15, 2000* (State Scientific Center of Russian Federation - Institute for Physics & Power Engineering, (SSC RF IPPE), Obninsk, Russia, 2000) pp. 72-82.
5. Yu.S. Zamiatnin, I.N. Safina, E.K. Tutnikova *et al.*, Atomn. Ener. **4**, 337 (1958).
6. V.Ya. Baryba, N.V. Kornilov, O.A. Sal'nikov, *Fission prompt neutron spectrum of ^{238}U for energy 14.3 MeV* (in Russian). Preprint FEI-947, 1979.
7. N.V. Kornilov, B.V. Zhuravlev, O.A. Salnikov *et al.*, in *Proceedings of the 5th Conference on Neutron Physics, Kiev, September 15-19, 1980*, Vol. **2** (TsNIIAtominform, Moscow, 1980) pp. 44-49.
8. N.V. Kornilov, Yad. Konst. **4**, 46 (1985), (translated in: INDC(CCP)-336, (IAEA, Vienna, 1991) p. 71).
9. I. During, H. Marten, A. Ruben, D. Seeliger, in *Proceedings of the Consult. Meeting, Vienna 1990*, INDC(NDS)-251 (IAEA, Vienna, 1991) pp. 159-181.
10. M.I. Svirin, G.N. Lovchikova, A.M. Trufanov, Yad. Fyz. **60**, 818 (1997).
11. J.W. Negele, S.E. Koonin, P. Moller, J.R. Nix, A.J. Sierk, Phys. Rev. C **17**, 1098 (1978).
12. Y. Boneh, Z. Fraenkel, Phys. Rev. C **10**, 893 (1974).
13. C. Budtz-Jorgensen, H.-H. Knitter, Nucl. Phys. A **490**, 307 (1988).
14. D. Hilscher, H. Rossner, Ann. Phys. (Paris) **17**, 471 (1992).
15. D.C. Madland, J.R. Nix, Nucl. Sci. Eng. **81**, 213 (1982).
16. T. Kawano, T. Ohsawa, M. Baba, T. Nakagawa, Phys. Rev. C **63**, 034601 (2001).
17. V.M. Maslov, Yu.V. Porodzinskij, A. Hasegawa, M. Baba, N.V. Kornilov, A.B. Kagalenko, in *Proceedings of the 10th International Seminar on Interaction of Neutrons with Nuclei, May 26-28, 2002, Dubna* (JINR, Russia, 2003).
18. V.M. Maslov, in *Nuclear Reaction data and Nuclear Reactors, Trieste, Italy, 2000*, (ICTP, 2001) p. 231.
19. E. Almen, E. Holmgvist, T. Wiedling, *Nuclear data for reactors*, in *Proceedings of the II International Conference on Nuclear Data for Reactors, Helsinki, 15-19 June 1970*, Vol. **2** (IAEA, Vienna, 1970) p. 183.
20. H.H. Knitter, Z. Phys. **244**, 358 (1971).
21. E. Bernard, A.T.F. Ferguson *et al.*, Nucl. Phys. **71**, 228 (1965).
22. V.Ya. Baryba, B.V. Zhuravlev, N.V. Kornilov *et al.*, Atomn. Ener. **43**, 266 (1977).
23. A. Bertin, C. Clageux, *Proceedings of the 3rd Conference on Neutron Cross-Sections and Technology, Knoxville, USA, 15-17 March, 1971* (US Government Printing Office, Washington, DC, 1972) p. 286.
24. Yu.A. Vasil'ev, Yu.S. Zamiatnin *et al.*, Sov. Phys. JETP **38**, 671 (1960).
25. J. Frehaut, NEANDC(E)-238/L, INDC(FR)-67/L, 1986; J.W. Negele, S.E. Koonin, P. Moller, J.R. Nix, A.J. Sierk, Phys. Rev. C **17**, 1098 (1978).
26. N.V. Kornilov, A.B. Kagalenko, F.-J. Hambsch, Yad. Fiz. **62**, 209 (1999).
27. V.V. Malinovskij, Yad. Konst. **2**, 25 (1987).
28. V.P. Eismont, Atomn. Ener. **19**, 113 (1965).
29. H. Marten, D. Seeliger, J. Phys. G: Nucl. Phys. **14**, 211 (1988).
30. J.W. Behrens, G.W. Carlson, Nucl. Sci. Eng. **63**, 250 (1977).
31. B.I. Fursov *et al.*, Sov. J. At. Energy **43**, 808 (1978).
32. J.W. Meadows, Nucl. Sci. Eng. **58**, 255 (1975).
33. P.E. Vorotnikov, S.M. Dubrovina, G.A. Otroshchenko *et al.*, Yad. Phys. Issled. **12**, 22 (1971).
34. I.D. Alkhazov, V.P. Kasatkin, O.I. Kostochkin *et al.*, *Neutron Physics, Proceedings All-Union Conference*, Vol. **4** (Tsniiatominform, Moscow, 1973) p. 13.
35. P.W. Lisowski, A. Gavron, W.E. Parker *et al.*, *Proceedings of the Specialists' Meeting on Neutron Cross-Section Standards for the Energy Region above 20 MeV, Uppsala, Sweden, May 21-23, 1991* (OECD, Paris, 1991) p. 177.
36. J.D. Knight, R.K. Smith, B. Warren, Phys. Rev. **112**, 259 (1958).
37. N.V. Kornilov, O.A. Sal'nikov *et al.*, *Voprosi Atomnoi Nauki i Tehniki (VANT)*, Ser. Yad. Konst. **1** (45), 33 (1982).
38. A. Ackerman, B. Anders, H. Borman, *Proceedings of the Conference on Nuclear Cross-Sections and Technology, Washington D.C., March 3-7, 1975*, CONF-750303, Vol. **2** (US National Bureau of Standards, 1975) p. 425.
39. S. Nagy, K.F. Flynn *et al.*, Phys. Rev. C **17**, 163 (1978).
40. L.R. Veeser, E.D. Arthur, *Proceedings of the International Conference on Neutron Physics and Nuclear Data* (OECD, Harwell, 1978) p. 1054.
41. J. Frehaut, G. Mosinski, *Proceedings of the Confernce on Nuclear Cross-Sections and Technology, Washington D.C., March 3-7, 1975*, CONF-750303, Vol. **2** (US National Bureau of Standards, 1975) p. 855.
42. J. Frehaut, A. Bertin, R. Bois, Nucl. Sci. Eng. **74**, 29 (1980).
43. A.A. Filatenkov, S.V. Chuvaev, V.N. Aksenov *et al.*, INDC(CCP)-402 (IAEA, Vienna, 1997).
44. Chou You-Pu, Report HSJ-77091,7810.
45. S. Bjornholm, J.E. Lynn, Rev. Mod. Phys. **52**, 725 (1980).
46. L.G. Moretto, Nucl. Phys. A **180**, 337-362 (1972).
47. H.-H. Knitter, U. Brosa, C. Budtz-Jorgensen, *Neutron and Gamma Emission in Fission, The Nuclear Fission Process*, edited by C. Wagemans (CRC Press Inc., 1991) pp. 497-553.
48. N.V. Kornilov, A.B. Kagalenko, in *Proceedings of the II International Seminar on Interaction of Neutrons with Nuclei, April 26-28, 1994, Dubna, Russia* (Joint Institute for Nuclear Research, Dubna, Russia, 1994) p. 116.